Scanning Microscopy

Volume 6 | Number 1 Article 7

3-6-1992

Image Processing Procedures for Analysis of Electron Back Scattering Patterns

N. C. Krieger Lassen
Risø National Laboratory

D. Juul Jensen
Risø National Laboratory

K. Conradsen
The Technical University of Denmark

Scanning Microscopy, Vol. 6, No. 1, 1992 (Pages 115-121) 0891-7035/92$5.00+.00
Scanning Microscopy International, Chicago (AMF O'Hare), IL 60666 USA

IMAGE PROCESSING PROCEDURES FOR ANALYSIS OF ELECTRON BACK SCATTERING PATTERNS

N.C. Krieger Lassen[1*], D. Juul Jensen[1] and K. Conradsen[2]

[1]Materials Department, Risø National Laboratory, P.O.Box 49, DK-4000 Roskilde, Denmark.
[2]The Institute of Mathematical Statistics and Operations Research, The Technical University of Denmark, DK-2800 Lyngby, Denmark.

(Received for publication November 22, 1991, and in revised form March 6, 1992)

Abstract

At present, computer-aided Electron Back Scattering Pattern (EBSP) analysis often requires large amounts of operator time if statistically reliable measurements are needed. This paper presents ways to automatically detect and localize bands in EBSPs and thereby enable fully automatic EBSP analysis. The main focus will be on a procedure using a modified Hough transform by which more than 12 bands in a typical EBSP can be detected and localized. This procedure seems as effective and reliable for extracting the bands of EBSPs as any human operator. The performance of this procedure is compared with that of other image processing procedures.

Key Words: Electron back scattering patterns, backscattered electrons, image processing, crystallographic orientation, Hough transform, line detection, automatic analysis, electron diffraction, computer procedure.

*Address for correspondence:
Niels C. Krieger Lassen
Materials Department
Risø National Laboratory
DK-4000 Roskilde, Denmark
Telephone No.: +45 42 37 12 12 ext. 5711
FAX No.: +45 42 35 11 73

Introduction

With knowledge of the location of bands in electron backscatter diffraction patterns (EBSPs) it is possible to measure lattice orientations of individual grains (Dingley *et al.*, 1987; Venables *et al.*, 1976; Young and Lytton, 1972). Until now the location of bands has required the time and attention of an operator. Since some applications of the EBSP technique need lattice orientations from thousands of grains it is of great interest to eliminate the need of an operator by locating the EBSP-bands automatically.

This paper presents a method based on the Hough transform (Hough, 1962) by which information about the location of bands in EBSPs can be extracted. This method enables the detection and localization of more than 12 bands with high precision in a typical EBSP obtained with our equipment (a JEOL 840 SEM and a CCD very-low-light camera mounted in the side port). One feature of the method is that it requires very little preprocessing of the image because it exploits the fact that the EBSP-bands have higher intensities than the background. Another feature of the method is that no a priori information about the expected bandwidths is needed. The output information is simply the position of the center lines of EBSP bands.

The performance of this procedure is compared with the performance of procedures using the traditional Hough transform and the Burns algorithm (Burns *et al.*, 1986) used by Wright and Adams (1991).

Preprocessing of the EBSP Image

A sample of an EBSP image with a resolution of 480x512 pixels is given in Fig. 1. EBSP images contain a significant amount of background noise and variation in the background intensity level. This background can be approximated for a given sample by the image obtained with the electron beam scanning over several different crystallites. This background image B(x,y) is subtracted from the original image I(x,y):

$$I_1(x,y) = I(x,y) - B(x,y) \quad (1)$$

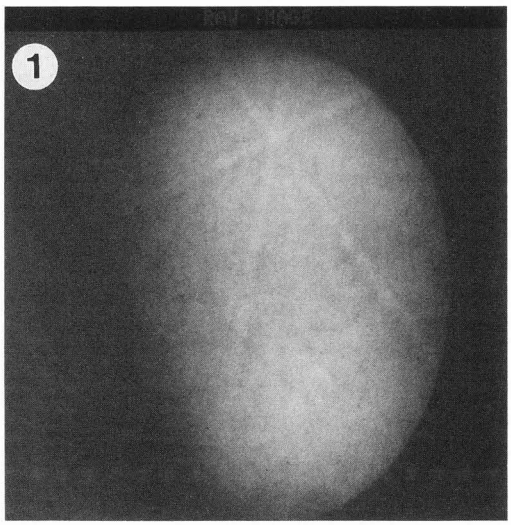

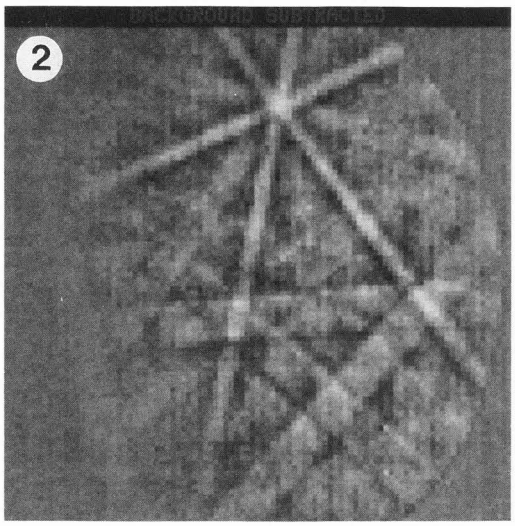

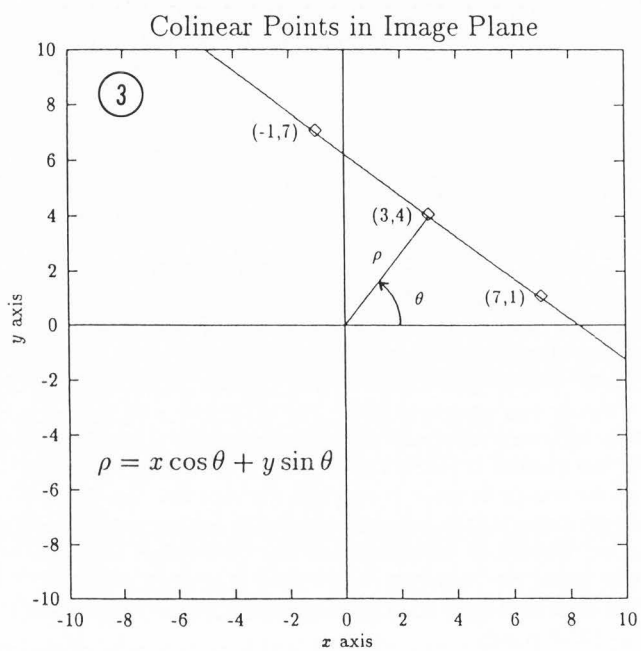

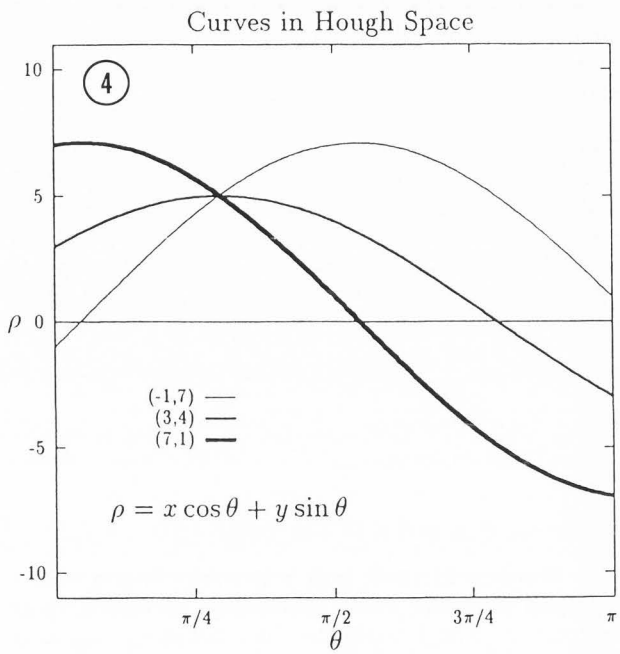

Fig. 1. EBSP image obtained from commercially pure aluminium. [480x512 pixels].

Fig. 2. Image obtained by first subtracting a background image (average from many different crystallites). Then an 400x400 image is taken from the center and the resolution is reduced by averaging over 4x4 pixel blocks. Finally a low pass filtered version of the image is subtracted. [100x100 pixels].

Fig. 3. Illustration of the so-called *normal parameterization* of straight lines. A line is specified by the angle θ of its normal and its algebraic distance ρ from the origin.

Fig. 4. Sinusoidal curves in Hough space (parameter space) corresponding to the three collinear points in Fig. 3. The common intersection point corresponds to the parameters of the line on which these three points lie.

From the center of $I_1(x,y)$ a 400x400 image is extracted. This image is subsequently reduced to a 100x100 image I_2 by averaging over 4x4 pixel blocks. This is done to reduce computational costs and does not seem to reduce the amount of (essential) information in the image. In many cases the I_2 image still has some background intensity variation. This is due to the fact that the background intensity in EBSPs varies somewhat from one grain to another. To reduce this variation in background intensity a low pass filtered version of I_2 is created by first reducing I_2 to a 20x20 image by averaging over 5x5 pixel blocks and secondly by enlarging this image to 100x100 pixels using bilinear interpolation (Rosenfeld and Kak, 1982). This is a relatively easy way to create a heavily low pass filtered (i.e., blurred) version of an image. This low pass filtered image is then subtracted from I_2:

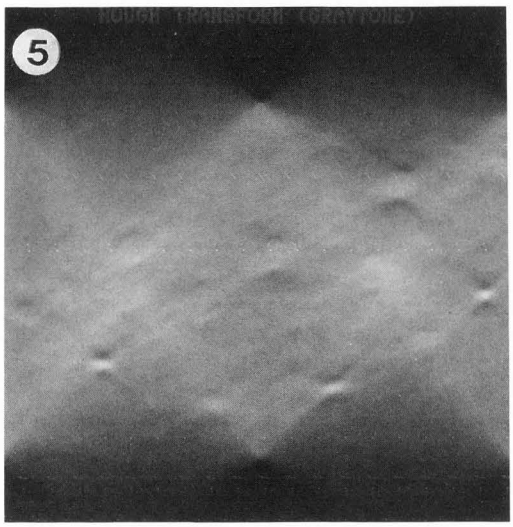

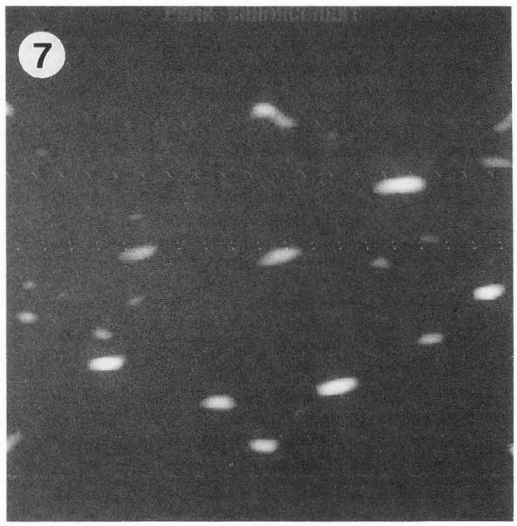

Fig. 6

-2	-2	-2	-4	-7	-10	-14	-10	-7	-4	-2	-2	-2
-2	0	-1	-2	-4	-7	-10	-7	-4	-2	-1	0	-2
-2	0	0	0	0	-3	-7	-3	0	0	0	0	-2
-2	0	2	2	1	2	-1	2	1	2	2	0	-2
-2	0	2	4	4	7	9	7	4	4	2	0	-2
-2	0	2	5	7	9	10	9	7	5	2	0	-2
-2	0	2	5	8	9	11	9	8	5	2	0	-2
-2	0	2	5	7	9	10	9	7	5	2	0	-2
-2	0	2	4	4	7	9	7	4	4	2	0	-2
-2	0	2	2	1	2	-1	2	1	2	2	0	-2
-2	0	0	0	0	-3	-7	-3	0	0	0	0	-2
-2	0	-1	-2	-4	-7	-10	-7	-4	-2	-1	0	-2
-2	-2	-2	-4	-7	-10	-14	-10	-7	-4	-2	-2	-2

Fig. 5. The Hough space after transformation of the image of Fig. 2. Peaks in Hough space correspond to lines in the image plane. [180x180 pixels].

Fig. 6. Butterfly-mask designed for enhancement of peaks in Hough space (13x13 elements).

Fig. 7. The result of filtering Hough space (Fig. 5.) using the butterfly-mask of Fig. 6. Notice the enhancement of peaks. [180x180 pixels].

$$I_3(x,y) = I_2(x,y) - \text{low pass } I_2(x,y) \quad (2)$$

The I_3 image corresponding to Fig. 1 is given in Fig. 2.

The Hough Transform for Line Detection

The Hough transform (Hough, 1962; Duda and Hart, 1972; Ballard and Brown, 1982) provides a technique for deriving the parameters of a straight line. It has been widely discussed in the literature, including theoretical aspects and efficient hard- and software implementations (for a survey see Illingworth and Kittler, 1988). The Hough transform extracts **global** lines and gives good results in the presence of noise. This makes it an obvious choice for extracting bands in EBSPs.

The set of lines in the picture plane constitutes a two-parameter family. In the context of the Hough transform the so-called *normal parameterization* is the one most often preferred:

$$x\cos\theta + y\sin\theta = \rho,\ \theta \in [0;\ \pi]\ \rho \in [-R;\ R] \quad (3)$$

This parameterization specifies a straight line by the angle θ of its normal and its algebraic distance ρ from the origin (Fig. 3). R is the distance from the origin to the corners of the image. The advantage of this parameterization when compared with the traditional slope-intersect parameterization is that the parameters are bounded.

A quantization of the parameter space (or Hough space, Fig. 4) is introduced and used as an accumulator array $H(\theta,\rho)$ when performing the Hough transformation on the image $I(x,y)$:

For each pixel (x_i,y_i):

Add $I(x_i,y_i)$ to all cells in $H(\theta,\rho)$ along the curve

$$\rho = x_i\cos\theta + y_i\sin\theta \quad (4)$$

In this way all points in the image plane (x_i,y_i) are transformed to sinusoidal curves (4) in Hough space. A point in Hough space (θ_i,ρ_i) corresponds to a unique straight line in the image plane. It is easy to show that collinear point in the image plane will be transformed to curves intersecting in a common point in Hough space corresponding to the parameters of the line on which they lie. The Hough transform thus converts the difficult problem of detecting global lines into a more easily solved problem of detecting peaks in parameter space.

The Hough transform can be interpreted as the end product of a process of accumulating "votes" in $H(\theta,\rho)$ from all pixels in the input image. Each pixel (x_i,y_i) gives $I(x_i,y_i)$ votes to all possible lines in the image passing through (x_i,y_i) since the parameters of these lines are determined from the curve (4). Points in Hough space receiving high counts of votes are likely to correspond to lines in the image plane.

The Hough transform is usually applied to binary images obtained by using a threshold value on the gradient of the original image. In this case only pixels having the value 1 (potential line points with high gradient values) need to be considered. Because the edges of EBSP bands are very unsharp, traditional edge detection schemes (Rosenfeld and Kak, 1982) are not very successful. Instead of using a tresholded gradient image as input to the Hough transform we simply use the graytone image $I_3(x,y)$ as input. This way we exploit the fact that the bands in EBSPs have higher intensity than the background. The intensity of each pixel $I_3(x_i,y_i)$ is used as a measure of evidence for a line passing through the pixel. The only problem with this approach is that the width of the EBSP bands results in a spreading of the corresponding peaks in Hough space.

The result of Hough transforming the image of Fig. 2 is given in Fig. 5. We found that a quantization of the Hough space in 180x180 cells gave good results.

The next step of the process is to locate the peaks in Hough space. Several authors have considered the spreading of peaks that occurs in Hough space (Van Veen and Groen, 1981; Leavers and Boyce, 1987). They have shown that all peaks have a characteristic butterfly-like shape and have derived formulas specifying peak spread in the ρ-direction. This spreading is directly proportional to line width. Inspired by Leavers and Boyce (1987) we designed a mask (Fig. 6) appropriate to detect and enhance peaks corresponding to bands of average size. Ideally one should use different masks for enhancing peaks corresponding to bands of different widths. We found that the mask of Fig. 6 was a compromise leading to good results. The result of applying this 13x13 convolution mask to the image of Fig. 5 is given in Fig. 7.

In the next step of the procedure local maxima of the filtered Hough space are found by a simple search algorithm. The maxima are ordered according to peak intensity and transformed into lines in the image plane. The resulting lines are given in Fig. 8.

The last step of the procedure adjusts the detected bands by exploiting the fact that we (*a priori*) know that some bands must intersect in a common point (corresponding to poles). Bands that almost intersect in a common point are grouped together. These groups naturally consist of at least three bands and the group containing the most bands is considered first. The problem of finding the optimal intersection point (x_{int},y_{int}) of the bands (θ_i,ρ_i) in a group can be considered as the problem of fitting a sinusoidal curve (3) to the points (θ_i,ρ_i). This is a simple linear curve fitting problem which we solve using the weighted least squares method. The weights we use w_i are the intensities of the corresponding peaks (maxima) in the filtered Hough space. Finally we adjust the bands in a group by projecting the corresponding points (θ_i,ρ_i) on to the fitted curve ((3) with $(x,y) = (x_{int},y_{int})$). After adjusting the bands of the group with the most bands we proceed to the group with the next most bands and so on. When a band is encountered that has already been adjusted in a former step of the process we fix the band by the two points that it must go through.

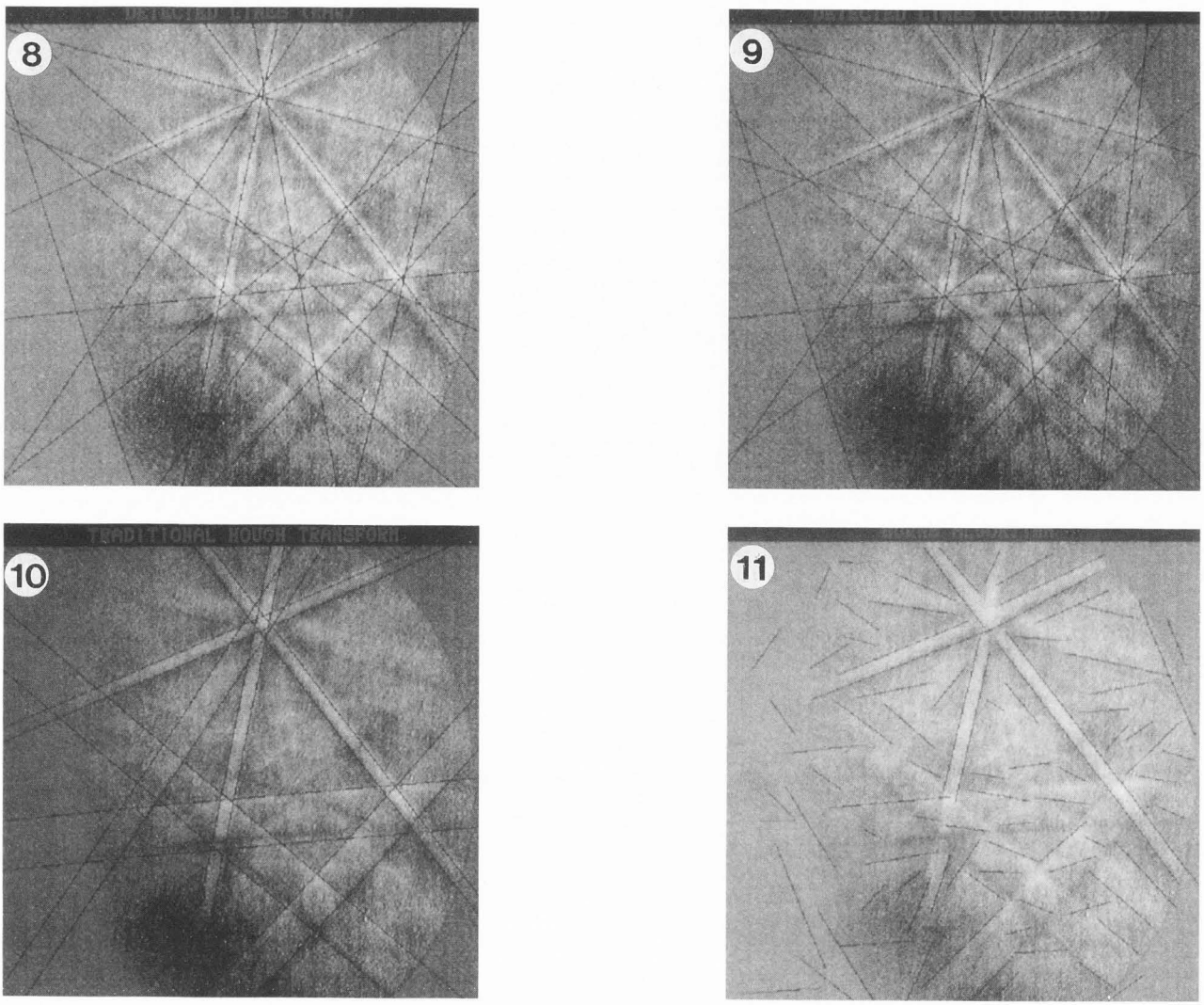

Fig. 8. The resulting lines after localizing local maxima in the filtered Hough space (Fig. 7). [400x400 pixels].

Fig. 9. The resulting lines after localizing local maxima in the filtered Hough space (Fig. 7) and exploiting that some bands must intersect in common poles. [400x400 pixels].

Fig. 10. Lines found by the traditional Hough transform. [400x400 pixels].

Fig. 11. Line segments found by the Burns algorithm. [400x400 pixels].

This band fitting scheme improves the accuracy of the location of weak and broad bands. The result of the process is illustrated in Fig. 9. Notice that the resulting lines are drawn upon the I_1 image (400x400) to illustrate location accuracy.

Alternative Methods

An obvious alternative to the procedure given above is to concentrate on locating the edges of the EBSP bands. Edge detection is a well established field in image processing (Rosenfeld and Kak, 1982) and numerous methods have been proposed. The traditional methods are based on calculating the intensity gradient of the image and following this by peak detection. We tested a more refined approach to edge detection proposed by Deriche (1987). This edge detection method is optimal according to some criteria for effective edge detection and localization.

Edge detectors only give a local measure of the probability of a pixel being part of an edge. One way to extend this local edge information into global edge information is to threshold the edge detected image and apply the Hough transform (this is the standard way of using the Hough transform). Using this approach we obtained very poor results. Instead, we tried using the output of the edge detector directly as input to the Hough transform. As in the procedure described above we filtered

Hough space to enhance peaks but this time used the mask proposed by Leavers and Boyce (1987):

$$\begin{matrix} 0 & -2 & 0 \\ 1 & 2 & 1 \\ 0 & -2 & 0 \end{matrix}$$

Using this approach we were able to locate about 5 bands. The result is given in Fig. 10. This procedure is able to extract information about band width and is just as time consuming as the procedure described above.

Another way to extend local edge information into more global edges is to use local orientation information. This is done by the Burns algorithm (Burns *et al.*, 1986) that was used for EBSPs by Wright and Adams (1991). This algorithm first estimates local gradient orientation by using the result of convolving the image with two masks sensitive to edges in the x and y direction. Gradient orientation is then coarsely quantized into a set of ranges ("buckets") which serve as pixel labels. Adjacent pixels having identical bucket labels are grouped into so-called line support regions and a line is fitted to each region. The result of applying the Burns algorithm to the image I_3 is given in Fig. 11. Our version of the Burns algorithm is similar to the one used by Wright and Adams (1991). From Fig. 11 it is easy to see that some postprocessing is needed to extract the location of the bands. Wright and Adams (1991) have proposed some postprocessing steps that lead to good results. Some of these steps need *a priori* information about the minimum and maximum theoretical bandwidth that can be expected for the bands in the EBSP.

Results

We tested the procedure described in the section **The Hough Transform for Line Detection** on 25 patterns obtained from fully recrystallized commercially pure aluminium (99.4%) with an average grain size of 25 μm. As the procedure is supposed to substitute the work of an operator its reliability and accuracy are simply judged by the human eye. We found that the image processing procedure enabled the detection of 12 to 16 bands with an average of 14. The procedure actually seemed able to compete with the human eye in the ability to detect bands. In some cases bands were detected that could not actually be seen by the eye but should be there (according to pattern simulations). Furthermore the accuracy of the locations of bands seemed as good as one could expect from the work of any operator.

Using a HP-9000/750 computer the bands of a pattern can be located in approximately 6 seconds. On a 80486 33 MHz personal computer (PC) the calculations are performed in about 40 seconds.

Summary

This paper has presented a procedure for extracting the bands of EBSPs that seems as effective and reliable for this job as any human operator. The procedure requires no *a priori* information about the sample in question and is relatively simple to implement. Furthermore the parameters of the procedure need only to be adjusted once and are not sensitive to different samples. Another advantage of the method is that it is insensitive to bands corresponding to higher order reflections.

The next step is of course to use the detected lines as input to an EBSP analysis procedure like the one described by Juul Jensen and Schmidt (1990). This procedure is able to simulate an EBSP pattern using the input of at least 2 bands. Using for instance 3 bands as input the first simulation will be correct for 80 % of the EBSPs. By using the remaining 9-13 bands identified by the image processing procedure it is a simple task to check if a simulation is correct. We are currently working on combining the image processing procedure with the EBSP analysis procedure in a sensible way. This will lead to a fully automatic EBSP analysis procedure.

References

Ballard DH, Brown CM (1982) Computer Vision. Prentice Hall, 123-130.

Burns JB, Hanson AR, Riseman EM (1986) Extracting straight lines. IEEE Transactions on Pattern Analysis and Machine Intelligence, **8**, 425-455.

Deriche R (1987) Using Canny's criteria to derive a recursively implemented optimal edge detector. International Journal of Computer Vision, **6**, 409-433.

Dingley DJ, Longden M, Weinbren J, Alderman J (1987) On-line analysis of electron back scatter diffraction patterns. I. Texture analysis of zone refined polysilicon. Scanning Microsc., **1**, 451-456.

Duda RO, Hart PE (1972) Use of the Hough transformation to detect lines and curves in pictures. Communications of the ACM, **15**, 11-15.

Hough PVC (1962) Method and means for recognizing complex patterns. U.S. Patent 3,069,654, Dec. 18, 1962.

Illingworth J, Kittler J (1988) A Survey of the Hough transform. Computer Vision, Graphics and Image Processing, **44**, 87-116.

Juul Jensen D, Schmidt NH (1990) An automatic online technique for determination of crystallographic orientations by EBSP. In: Recrystallization '90, Chandra T (ed.), The Materials Society, Warrendale, PA, 219-224.

Leavers VF, Boyce JF (1987) The Radon transform and its application to shape parameterization in machine vision. Image and Vision Computing, **5**, 161-166.

Rosenfeld A, Kak AC (1982) Digital Picture Processing. Academic Press, Orlando, 57-190.

Van Veen TM, Groen FCA (1981) Discretization

errors in the Hough transform. Pattern Recognition, **14**, 137-145.

Venables JA, Harland CJ, bin-Jaya R (1976) Crystallographic orientation determination in the S.E.M. using electron back-scattering patterns and channel plates. In: Developments in electron microscopy and analysis. Academic Press, London, 101-104.

Wright SI, Adams BL (1991) Automatic Analysis of Electron Backscatter Diffraction Patterns. Metallurgical Transactions, in press.

Young CT, Lytton JL (1972) Computer generation and identification of Kikuchi projections. Journal of Applied Physics, **43**, 1408-1417.

Discussion with Reviewers

S. Wright: In Figures 5 and 7 it is clear that some of the peaks are not due directly to the diffraction bands but due to artifacts in the Hough transform (because a square image is used). How do you distinguish the true peaks arising from bands in the diffraction patterns with those peaks that are simply artifacts of the Hough transform.

Authors: The presence of the artifacts you mention are not really a consequence of the fact that we use a square image, but the location and appearance of the artifacts are. It is more accurate to say that the artifacts are a consequence of the finite size of the image. These artifacts are most clearly seen if the Hough transformation is applied to a uniform image (all pixels having the same value or color) in which case the result will **not** be a uniform Hough space. The reason for this is really quite obvious: A cell in the quantized Hough space corresponds to a line in the input image and this cell will only receive contributions to the total count of that cell from points in the image lying on the corresponding line. Since the input image will always be finite the number of points that contribute to a given cell in Hough space will always vary according to the length of that part of the line that falls inside the image. The artifacts in Hough space are therefore easily described for a given shape of the image (the retina). For each cell in Hough space it is straight forward to calculate the length of that part of the corresponding line that falls inside the given image. By dividing the total count in each cell in Hough space by the calculated length of the corresponding line (inside the image) the artifacts are eliminated.

This procedure was tested but we concluded that it did not improve the results. This is because the subsequent filtering of Hough space removes most of these artifacts. The only artifacts that remains after the filtering can be seen in Fig. 7 at points corresponding to $\theta = 0°, 90°, 180°$ and $\rho = \pm 50$. Since the input image is square and of size 100x100 pixels these artificial peaks correspond to the borderlines of the image. In the process of peak detection we simply ignore peaks around these special points in Hough space.

S. Wright: How does the quality of the EBSPs affect the ability of the algorithm to correctly identify the diffraction bands.

Authors: Our experience has indicated that the algorithm is very robust especially to noise (randomly distributed, spatially) and to blurring of the EBSP. The contrast between bands and background seems to be the most important factor for the effectiveness of the algorithm but quantified results are needed to support these observations. In general, we have found that the algorithm is able to compete with the human eye in the ability to detect and localize bands in EBSPs.